Materials Research. 2013; 16(2): 315-321
DOI: 10.1590/S1516-14392012005000184

Analysis of Effective Thermal Conductivity for Mineral Cast Material Structures with Varying Epoxy Content Using TPS Method

A. Selvakumar*, P. V. Mohanram

Department of Mechanical Engineering, PSG College of Technology, Coimbatore, India

Received: June 6, 2012; Revised: October 5, 2012

Conventionally, cast iron is the material used for high speed machine tool structures. As an alternate material to improve the structural properties, composite materials are being used, which are known to exhibit excellent thermal and mechanical properties. While selecting an alternate material, thermal conductivity is an important thermo physical property of the material that should be studied. A resin composite material has a lesser thermal conductivity and its thermal properties vary with the composition of the mixture. A material with lower thermal conductivity will have higher heat concentration within the structure, which may result in structural deformation. In this analysis, epoxy granite, a material which is tested to exhibit excellent mechanical properties has been selected to study its thermal properties. Tests are carried out using Transient Plane Source (TPS) method, on eight samples with varying volume fraction of epoxy content in the range 10-24%. It is observed that, the effective thermal conductivity decreases with an increase in epoxy resin content in the mixture because the resin content increases interfacial resistance between particles. Hence, lower epoxy content in the mixture that maximizes the effective thermal conductivity while maintaining good mechanical properties is to be selected.

Keywords: *thermal conductivity, composite material, resin composite*

1. Introduction

In high speed machine tools, the material used in its structure play a major role in the productivity of the machine and the accuracy of the parts manufactured. They also influence the static and dynamic stiffness, mass, modal and thermal properties of the machine tools. The material selected for the machine tool structures must possess excellent mechanical and thermal properties which would reduce the geometric and thermal errors and improve the accuracy of the parts manufactured. Cast iron is the most preferred conventional structural material used in manufacturing precision machine tool structures, as it has excellent damping properties which minimize the dynamic loads and its high quality to price ratio. However, while working at high operating speeds, thermal energy generated is transported through the structural components. Due to high thermal expansion coefficients, cast iron structures deflect causing positional errors between the structural parts. Studies indicate that machine tool structures having low mass and high damping compared to conventional materials improves productivity[1,2]. Hence recent research on high speed precision machine tool structures aims at developing an alternate composite material which exhibit good thermal characteristics along with its excellent mechanical properties.

Composite materials are emerging as an excellent alternative to conventional cast iron structures due to their good chemical resistance, ease of production, workability, high strength-to weight ratio, low thermal conductivity, and excellent damping properties. Research is being conducted on stone based concrete materials as alternatives for machine tool supporting structures. Polymer concretes like polyester concrete and epoxy concrete are two types of materials under study. Polymer concrete structures make use of polymer resin as its matrix material. In epoxy concrete epoxy resin is used as the binding element. The characteristics exhibited by polymer concrete structures were studied by varying the compositions of its ingredients in it[3-7]. It is proved that, the epoxy granite composites with 12% epoxy content in the mixture exhibit good damping and stiffness properties and strength, making it more preferable alternative material for precision machine tool structures.

In epoxy granite composite, which has two ingredients, effective thermal conductivity is an important physical property that has to be determined. Techniques that were used to determine the effective thermal conductivities can be classified as either steady state methods or transient methods. In steady state technique, a steady temperature gradient will build up over a known thickness of the sample. The major disadvantage of this technique is that it is a time consuming technique and requires a large sample size.

Transient Plane Source (TPS) techniques were developed to cover a large range of transport properties and to apply the technique to a larger range of materials. This is a fast technique which starts responding as and when the heat input signals are supplied to the sample. This technique has been used reliably to find effective thermal conductivity of materials such as, metal foams[8], fire resistive materials[9], hydrating cement pastes[10], HVFA mortars and concrete materials[11], insulation materials[12] and Silicone rubber

*e-mail: selshasan@yahoo.co.in

composites with different metallic and non metallic filler materials[13]. It is demonstrated that crushed particles will have a higher thermal conductivity than natural particles[14].

The goal of this study is to determine the effective thermal conductivity of epoxy-granite material using TPS method and also the effect of varying the volume fraction of epoxy content in the mixture on the effective thermal conductivity of the epoxy granite material, developed as an alternate material for machine tool structures.

2. Preparation of Test Samples

Eight pairs of test specimens are prepared as shown in Figure 1 by varying the volume fraction of epoxy content ranging between 10-24% in the mixture in intervals of 2%. The range for study is selected from the literature which indicates that, the preferable range of volume fraction of epoxy content in a mixture is 12%-20%, considering the strength and mechanical properties of the structure developed[15,16]. The mixtures selected for analysis in this study are given in Table 1.

The manufacturing details for the epoxy granite specimen with 12% epoxy content are as follows. The aggregate material (granite particles) amounts to 88% by weight of the mixture. The aggregate particle mixture consist of coarse (granite particle size 0.5-4 mm) to fine (particle size less than 0.5 mm) particles in the ratio 50:50. 12% by weight of the mixture is selected as binding material, consisting of epoxy resin (LY 556) and 2% by weight of resin as hardener (HY 951).

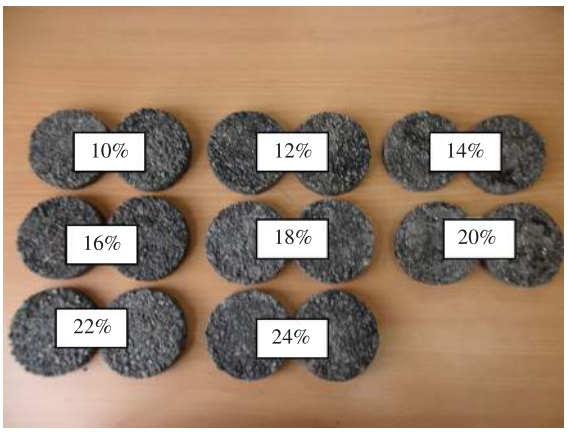

Figure 1. Test specimens with varying epoxy content.

Table 1. Composition of mixtures selected for analysis.

Sl. No	Composition
1	10% epoxy + 90% granite
2	12% epoxy + 88% granite
3	14% epoxy + 86% granite
4	16% epoxy +84% granite
5	18% epoxy + 82% granite
6	20% epoxy + 80% granite
7	22% epoxy + 78% granite
8	24% epoxy + 76% granite

The aggregates and the binding material are mixed thoroughly and then poured into a wooden pattern prepared of required size. The pattern fixed in a horizontal shaker is shaken well continuously to remove the air entrapped between the particles and for compact packing of materials. The test specimen is cured for 24 hours at room temperature. Other specimens are also prepared using the manufacturing technique discussed above.

The test specimen consists of two cylindrical blocks of radius 35 mm and thickness 12.8 mm. The densities of the samples are maintained at $2100 \pm 4\%$ kg.m^{-3}. To reduce the contact errors of thermocouple with unwanted surfaces, a 2 mm sheath is placed at the centre of the bottom block. The thermocouple is inserted through the sheath such that its tip just touches the center of the heater.

3. Experimental Setup

An experimental setup as shown in Figure 2, available in the fluid machinery lab of the mechanical engineering department has been used to find out the thermal conductivity of the samples using TPS method. The components of the set up consist of, a computer with LabVIEW 8.5 software, programmed to collect the temperature readings for every 30 seconds, from a J-type thermocouple in contact with the center point of a double spiral nickel wire heater kept between the samples. A SCXI 1303 DAQ card is used to interface the thermocouple with the computer. A 'ScientiFic' multiple power supply, PSD 3304 DC power supply unit are used to provide heat input to the heater.

The heater wire is made of 10μm thick, nickel metal wire, which is wound into a double spiral shape with twelve concentric circles and is well supported by a polymer film, called 'Kapton', which protects the shape of the coil while providing, good electrical insulation and mechanical strength to the heating coil.

A wooden cylindrical container with its inner surface well insulated with glass wool, to avoid any heat loss to the surroundings, is used to hold the specimen. The heater sandwiched between the specimens is firmly fixed between the wooden containers. The thermocouple connected to a Data acquisition (DAQ) card is inserted through a sheath in the bottom specimen and placed firmly such that it touches the center point of the heater. The DAQ card receives signals from the thermocouple and it is processed by a computer with LabVIEW 8.5 software.

A DC Power source is used to supply power to the heater. The time dependent temperature rise is noted down for every 30 seconds in a computer with LabVIEW programme.

4. Transient Plane Source Method

The TPS method has been developed to cover a large number of transport properties as possible and at the same time to apply the technique to a large number of materials. An external dc power source is used to supply constant voltage and current to the TPS heating coil, wound into the shape of a double spiral, so as to obtain a constant output power from it. The heat generated is dissipated into the testing material and the temperature rise is monitored by noting the resistive change in the element. The resistance

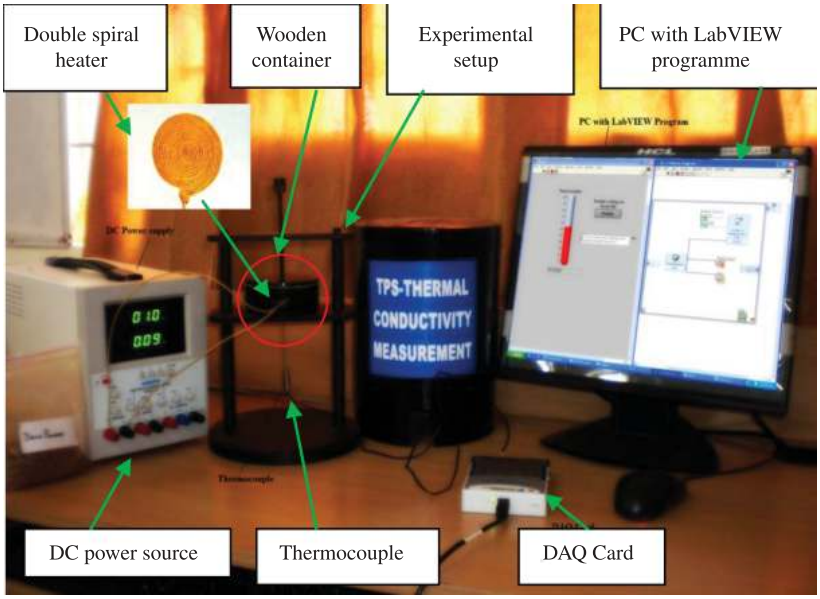

Figure 2. Experimental set up: TPS Method.

data points are used to set a relation between temperature (T) and time (x).

The heat conduction equation for an isotropic material independent of temperature is given by Equation 1[13,17],

$$\alpha\nabla^2 T + \frac{Q}{\rho c} = \frac{\partial T}{\partial t} \tag{1}$$

where, 'α' is the thermal diffusivity, Q (x,y,z,t) is the amount of heat released at (x,y,z and time, t) per unit volume and time, T(x,y,z,t) is the temperature at any point (x,y,z and t), 'ρ' and 'c' are the density and specific heat of the material respectively.

To understand the behaviour of heating coil used in TPM technique theoretically, the heat conduction Equation 1 is solved, assuming that the heating coil (hot disk) consists of a certain number of concentric ring heat sources located in an infinitely large sample. Since the hot disk is electrically heated, the increase in its resistance can be conveniently expressed as a function of time as given in the Equation 2[12].

$$R(t) = R_0\left[1 + \Omega\left\{\Delta T_i + \Delta T_{ave}(\tau)\right\}\right] \tag{2}$$

where, R_o is the resistance of the disk at time t = 0, Ω is the temperature coefficient of the resistivity (TCR). ΔT_i is constant temperature difference developed over the thin insulating layers covering two sides of the hot disk sensor material. ΔT_{ave} is the increase in temperature of sample surface on the other side of the insulating layer and facing the hot disk.

The temperature increase recorded by the sensor, derived from Equation 2, is given in Equation 3,

$$\Delta T_{ave}(\tau) + \Delta T_i = \frac{\left[\left\{\frac{R(t)}{R_0}\right\} - 1\right]}{\Omega} \tag{3}$$

Here, ΔT_i is a measure of the 'thermal contact' between the sensor and the sample surface; ΔT_i becomes constant after a short time 'Δt_i', estimated using Equation 4.

$$\Delta t_i = \frac{\delta^2}{\alpha_i} \tag{4}$$

Where, 'Δ' is the thickness of the insulating layer and 'α_i' the thermal diffusivity of the layer material. The variable time 'τ' is defined by Equation 5 for easy calculation of temperature rise,

$$\tau = \left[\frac{t}{\vartheta}\right]^{\frac{1}{2}} \tag{5}$$

where 't' is the time measured from the start of the transient recording and 'ϑ' is the characteristic time defined by Equation 6.

$$\vartheta = \frac{a^2}{\alpha} \tag{6}$$

where, 'a' is a constant measuring the overall size of the resistive pattern (equal to the radius of the sample in this study) and 'α' is the thermal diffusivity of the sample.

Nandi et al.[13], has solved the heat conduction Equation 1, for a hot disk with 'm' concentric rings, and obtained the temperature rise caused by hot disk sensor at any point 'r' as in Equation 7.

$$\Delta T(r,\tau) = \frac{P_0}{2\pi^{3/2} am(m+1)k\rho c}\int_0^{\tau}\frac{d\sigma}{\sigma^2}\times\sum_{l=1}^{m} l.\mathrm{e}^{\frac{-\left((r/a)^2+(l/m)^2\right)}{4\sigma^2}} I_0\left(\frac{rl}{2ma\sigma^2}\right) \tag{7}$$

where,

$I_0(x) = \frac{1}{2\pi}\int_0^{2\pi} e^{x\cos\theta}d\theta = \frac{1}{2\pi}\int_0^{2\pi} e^{x\sin\theta}d\theta$ is the 0^{th} order modified Bessel function of first kind, 'σ' is an integration variable defined as $\sqrt{\alpha(t-t')/a^2}$ and 'τ' is the dimensionless characteristic time ratio obtained from Equations 5 and 6.

The average temperature rise of the sensor is given by Equation 8

$$\overline{\Delta T}(\tau) = \frac{1}{L}\int_0^{2\pi} \Delta T(r,\tau) \sum_{n=1}^{m} \delta(r - \frac{na}{m}) r.d\theta \quad (8)$$

By solving Equations 7 and 8, the time-dependent average temperature increase over the surface of the sensor is obtained as given in Equation 9.

$$\Delta T_{ave}(\tau) = \left[\frac{P_0}{\pi^{\frac{3}{2}} ak}\right] D(\tau) \quad (9)$$

where, 'P_0' is the total output of power from the sensor, 'a' is the overall radius of the disk, 'k' is the thermal conductivity of the sample that is being tested and '$D(\tau)$' is a dimensionless time-dependent function with time.

A computational straight line plot is made between the recorded temperature increase versus '$D(\tau)$', which intercepts at ΔT_i. The slope given by Equation 10 is measured at experimental times much longer than Δt_i for accurate measurements. Slope = $\left[\frac{P_0}{\pi^{\frac{3}{2}} ak}\right]$ (10)

5. Results and Discussions

The *ln* (*x*) *vs*. *T* graph is plotted with the time (*x*) – temperature (*T*) values obtained for every thirty seconds using the LabVIEW programme. The plotted graph for the specimen with 12% epoxy resin content in the mixture is shown in Figure 3. The graph is an 'S' shaped curve with initial lag error and axial error regions. The initial lag error occurs due to the lag in temperature response due to heat transfer coefficient between the surface of heat source and testing material. The axial error occurs at higher temperatures at which the heat wave is absorbed or reflected by the testing material in axial direction. The slope of the curve, obtained after neglecting these error regions, is used to determine the effective thermal conductivity of the material. Trial and error method is adopted to determine the slope corresponding to the selected temperature, such that the values of thermal conductivity calculated from the slope is repeated within 2% error limit[10,12].

According to the transient plane source theory, the slope of the graph is given by Equation 10. Knowing the amount of heat supplied and the slope of the graph, the effective thermal conductivity of the test material is determined. The experiment is repeated three times and the average value of effective thermal conductivity is calculated. The experiment is repeated with other specimens prepared.

The variation of effective thermal conductivity (*k*) with temperature for each specimen is shown in Figure 4. It shows a decreasing trend for effective thermal conductivity with increase in temperature.

The effective thermal conductivity obtained at temperature 27 °C, for the specimens with varying epoxy content (% *x*) in the mixture ranging from 10-24%, is tabulated in Table 2 and plotted in Figure 5. It is observed that effective thermal conductivity decreases

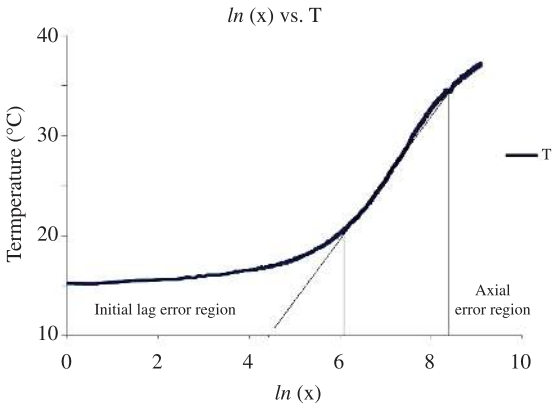

Figure 3. The initial lag error and axial error regions.

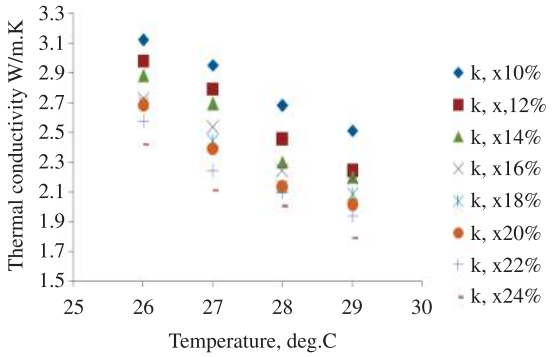

Figure 4. Variation of effective thermal conductivity with temperature (Power input: 1 W).

Table 2. Effective thermal conductivity obtained experimentally at T = 27 °C.

% Epoxy content in mixture	Effective thermal conductivity, k, W/m.K			Ave. effective thermal conductivity, keff
	k1	k2	k3	keff
10	3.0020	3.1317	2.7446	2.9594
12	2.4465	2.5475	3.3951	2.7964
14	2.4548	2.8359	2.7825	2.6911
16	2.5478	2.6365	2.4330	2.5391
18	2.5860	2.5368	2.1793	2.4340
20	2.5779	2.3253	2.1472	2.3501
22	2.5607	2.2296	1.9471	2.2458
24	2.0513	1.9978	2.2899	2.1130

with increase in epoxy content in the mixture. Neglecting the effect of size of crushed granite particles on effective thermal conductivity[16], the trend observed could be due to the presence of epoxy resin having very low thermal conductivity (0.363 W/m. K), between the granite particles. The use of epoxy resin for permanent bonding between the particles increases the interfacial resistance between the particles which in turn reduces the heat transfer between the surfaces[17] reducing the effective thermal conductivity. The effect of presence of other substances such as air or other foreign particles between the aggregates on effective thermal conductivity are neglected considering the steps taken during the manufacture of the sample such as 1) thorough cleaning and drying of aggregate particles removing any foreign particles in them 2) use of a horizontal shaker for proper filling of aggregates of different sizes without any void between particles and removal of air trapped between them increasing the compactness of the specimen prepared.

To validate the results found out experimentally using TPS method, three empirical models, namely the Hashin-Shtrikman (H-S) bounds[10], Jean Cote model[18] and geometric mean model are used[18].

The upper and lower Hashin-Shtrikman (H-S) bounds for effective thermal conductivity of two phase material are calculated using Equations 11 and 12 respectively[10].

For, $k_2 \geq k_1$

$$kl = k1 + \frac{x2}{\frac{1}{(k2 - k1)} + \frac{x1}{3k1}} \tag{11}$$

$$ku = k2 + \frac{x1}{\frac{1}{(k1 - k2)} + \frac{x2}{3k2}} \tag{12}$$

where, k_l and k_u are the upper and lower H-S bounds for effective thermal conductivity, k_1 and k_2 are the thermal conductivities of epoxy and granite materials respectively with volume fraction of epoxy resin (x_1) and granite particles ($x_2 = 1 - x_1$), in the test sample.

The upper and lower bounds of effective thermal conductivity are calculated by taking thermal conductivity for epoxy as 0.363 W/m.K as per the data given by the manufacturer and for the granite as 3.5 W/m.K. The H-S bounds, k_{upper} and k_{lower}, for varying concentration of epoxy and the experimental values of effective thermal conductivity are plotted in Figure 6. It is observed that, the effective thermal conductivity values obtained experimentally are well within the bounds.

The thermal conductivity values obtained experimentally for the samples are compared with the average values of H-S bounds and the values obtained using the correlation given by Jean Cote et al.[18] given in Equation 13 and by applying the geometric mean formula given in Equation 14.

$$k = \frac{(k_{2p}.k_s - k_f)(1-n) + k_f}{1 + (k_{2p} - 1)(1-n)} \tag{13}$$

Where, k_{2p} is the fluid to solid thermal conductivity ratio given by, $k_{2p} = 0.29\left(\frac{15k_f}{k_s}\right)^{\beta}$ and k_f and k_s are the thermal conductivity of fluid and solid respectively and β is the empirical parameter accounting structure effects on thermal conductivity.

$$k = (k_s)^{(1-n)} k_f{}^n \tag{14}$$

Where 'n' is the epoxy content in the mixture. The experimental values of effective thermal conductivities and the values calculated from the models are tabulated in Table 3.

A graphical comparison of experimental values with the values calculated using correlations, is shown in Figure 7. It is observed that, the effective thermal conductivity values obtained from this experimental study are very close to the values obtained by using correlations given by Jean Cote et al.[18] and geometric mean formula. The experimental values are very close to H-S bound average values at lower temperatures and vary within ±3% error limit at higher temperatures. This indicates the suitability of TPS method in the measurement of effective thermal conductivity for epoxy granite materials and in general for any two phase composite material.

The effective thermal conductivity values for the mineral cast epoxy granite material is found to be in the range of 2-3 W/m.K, which is twenty five times lesser than that of a conventional cast iron material, having a thermal conductivity value of 50 W/m.K. This shows that, the epoxy

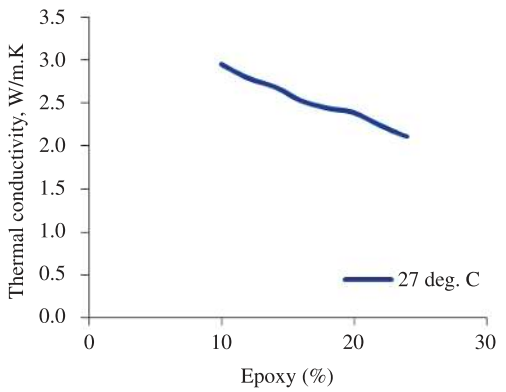

Figure 5. Variation of effective thermal conductivity with variation in epoxy content.

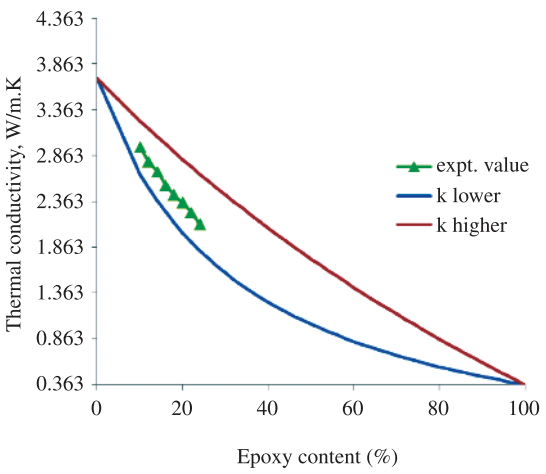

Figure 6. H-S bound chart for epoxy granite material.

Table 3. Effective thermal conductivity values from experimental and empirical methods.

% Epoxy content in mixture	HS bounds Ave	Cote et al. correlation	Geometric mean	This experimental study
10	2.9522	2.8889	2.9334	2.9594
12	2.8328	2.7566	2.8003	2.7964
14	2.7206	2.6323	2.6733	2.6911
16	2.6148	2.5152	2.5520	2.5391
18	2.5147	2.4047	2.4362	2.4340
20	2.4197	2.3003	2.3256	2.3501
22	2.3294	2.2014	2.2201	2.2458
24	2.2432	2.1077	2.1194	2.1130

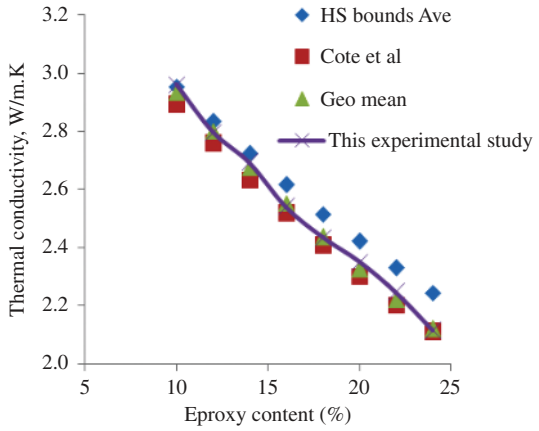

Figure 7. Comparison of effective thermal conductivity.

granite material will take a longer time to transport the heat generated in the structure. The heat transfer through the structure can be enhanced by selecting a mixture with lesser epoxy content, preferably in the range of 12-14% which maximizes the thermal conductivity without sacrificing its mechanical properties.

6. Conclusions

In the present work experiments are carried out, to determine the effective thermal conductivity of a mineral cast epoxy granite material using transient plane source techniques and to study the variation in effective thermal conductivity with varying volume fraction of epoxy content in the mixture. The measurement of effective thermal conductivity for eight samples with epoxy content varying in the range 10-24% is presented. A reduction in effective thermal conductivity is observed with increasing epoxy resin content in the mixture due to the presence of an interfacial material having low thermal conductivity (epoxy resin), which increases the interfacial resistance between the aggregate materials (granite particles). The effective thermal conductivity of the epoxy granite is observed to be in the range of 2-3 W/m.K, which is twenty five times smaller compared to conventional cast iron material for which the thermal conductivity is about 50 W/m.K. As a result, the supporting structure in a machine tool, made of epoxy granite material will reduce the thermal energy transport through it to other machine parts. However, an effective cooling method is required to carry away the heat stored in the supporting structure. A mixture with lesser epoxy content in the range 12-14% maximizes the effective thermal conductivity while maintaining the mechanical properties. By comparing the experimental effective thermal conductivity values with, empirical models such as H-S bounds, Cote et al.[18] and geometric mean correlations; it is observed that the experimental values are well within the range. TPS method is found to be quick and reliable technique for measuring effective thermal conductivity of composite materials.

References

1. Lee DG, Suh JD, Kim HS and Kim JM. Design and manufacture of composite high speed machine tool structures. *Composites Science and Technology*. 2004; 64:1523-1530. http://dx.doi.org/10.1016/j.compscitech.2003.10.021
2. Suh JD and Lee DG. Design and manufacture of hybrid polymer concrete bed for high-speed CNC milling machine. *International Journal of Mechanics and Materials in Design*. 2008; 4:113-121. http://dx.doi.org/10.1007/s10999-007-9033-3
3. Kim HS, Park KY and Lee DG. A study on the epoxy resin concrete for the ultra-precision machine tool bed. *Journal of Material Processing Technology*. 1995; 48:649-655. http://dx.doi.org/10.1016/0924-0136(94)01705-6
4. Orak S. Investigation of vibration damping on polymer concrete with polymer resin. *Cement and Concrete Research*. 2000; 30:171-174. http://dx.doi.org/10.1016/S0008-8846(99)00225-2
5. Piratelli-Filho A and Levy-Neto F. Behaviour of granite epoxy beams subjected to mechanical vibrations. *Materials Research*. 2010; 13(4):497-503. http://dx.doi.org/10.1590/S1516-14392010000400012
6. Rahman M, Mansur MA, Lee LK and Lum JK. Development of a polymer impregnated concrete damping carriage for linear guide ways for machine tools. *International Journal of Machine Tools and Manufacture*. 2001; 41(7):431-444. http://dx.doi.org/10.1016/S0890-6955(00)00072-9
7. Bruni C, Forcellese A, Gabrielli F and Simoncini M. Hard turning of an alloy steel on a machine tool with a polymer concrete bed. *Journal of Materials Processing Technology*. 2008; 202:493-499. http://dx.doi.org/10.1016/j.jmatprotec.2007.10.031

8. Rodríguez-Pérez MA, Reglero JA, Lehmhaus D, Wichmann M, De Saja JA and Fernández A. The Transient Plane Source technique (TPS) to measure thermal conductivity and its potential as a tool to detect inhomogeneities in metal foams. In: *Proceedings of the International Conference "Advanced Metallic Materials"*; 2003; Smolenice, Slovakia. Smolenice; 2003. p. 253-257.

9. Bentz DP. Combination of Transient Plane Source and slug calorimeter measurements to estimate thermal properties of fire resistive materials. *Journal of Testing and Evaluation*. 2007; 35(3):1-5.

10. Bentz DP. Transient plane source measurements of the thermal properties of hydrating cement pastes. *Materials and Structures*. 2007; 40:1073-1080. http://dx.doi.org/10.1617/s11527-006-9206-9

11. Bentz DP, Peltz MA, Duran Herrera A, Valdez P and Juarez CA. Thermal properties of high volume flyash mortars and concretes. *Journal of Building Physics*. 2011;34(3):263-275. http://dx.doi.org/10.1177/1744259110376613

12. Al-Ajlan SA. Measurements of thermal properties of insulation materials by using transient plane source technique. *Applied Thermal Engineering*. 2006; 26:2184-2191. http://dx.doi.org/10.1016/j.applthermaleng.2006.04.006

13. Nandi AK, Cingi C, Datta S and Orkus J. Experimental investigation on equivalent properties of particle reinforced silicone rubber: Improvement of soft tooling process. *Journal of Reinforced Plastics and Composites*. 2011; 30(17):1429-1444. http://dx.doi.org/10.1177/0731684411415888

14. Côté J and Konrad J-M. Assessment of structure effects on the thermal conductivity of two-phase porous geomaterials. *International Journal of Heat and Mass Transfer*. 2009; 52(3-4):796-804. http://dx.doi.org/10.1016/j.ijheatmasstransfer.2008.07.037

15. Mani P, Gupta AK and Krishnamoorthy S. Comparative study of epoxy and polyester resin-based polymer concretes. *International Journal of Adhesion and Adhesives*. 1987; 7(3):157-163. http://dx.doi.org/10.1016/0143-7496(87)90071-6

16. Piratelli-Filho A and Shimabukuro F. Characterisation of compression strength of granite-epoxy composites using design of experiments. *Materials Research*. 2008; 11(4):399-404. http://dx.doi.org/10.1590/S1516-14392008000400003

17. Incropera FP and Dewitt DP. *Fundamentals of heat and mass transfer.* 5th ed. Singapore: John Wiley and Sons Pte Ltd.; 2005. p. 93-95.

18. Côté J, Fillion M-H and Konrad J-M. Estimating hydraulic and thermal conductivities of crushed granite using porosity and equivalent particle size. *Journal of Geotechnical and Geo-Environmental Engineering*. 2011; 834-842. http://dx.doi.org/10.1061/(ASCE)GT.1943-5606.0000503